Supporting Information

Interface Engineering of 2D Dielectric Nanosheets for Boosting Energy Storage Performance of Polyvinylidene fluoride-Based Nanocomposites with High Charge-Discharge Efficiency

Hexing Liu[a], Jian Wang[b], Yunfan Wang[a], Zhonghui Shen[b], Xin Zhang[b], and Bao-Wen Li[a,*]

[a] *State Key Laboratory of Silicate Materials for Architectures, School of Materials Science and Engineering, Wuhan University of Technology, Wuhan 430070, China*

[b] *State Key Laboratory of Advanced Technology for Materials Synthesis and Processing, Center of Smart Materials and Devices, Wuhan University of Technology, Wuhan 430070, China*

* Corresponding author.

E-mail address: bwli@whut.edu.cn (B.-W. Li)

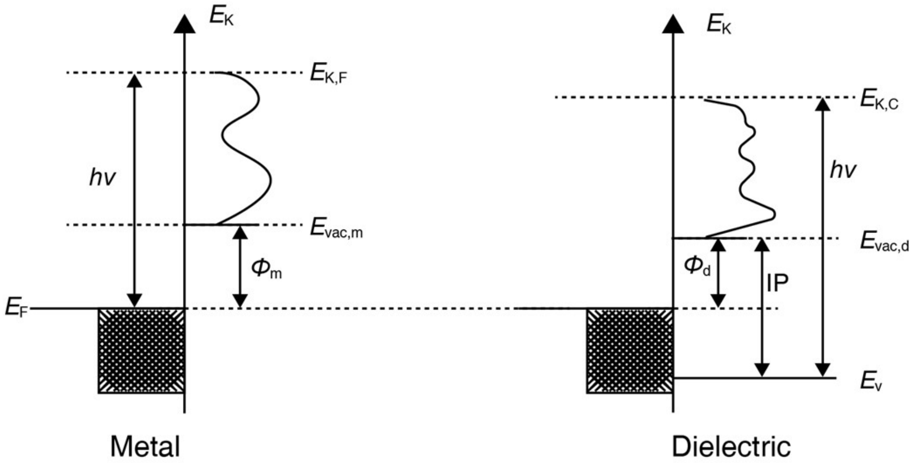

Figure S1. A schematic illustration depicting the E_v (Conduction Band) level measurement within coating layers using ultraviolet photoelectron spectroscopy (UPS). Notations used in the diagram include *hv* for ultraviolet photoelectron energy, E_k for the kinetic energy of the photoelectron, ϕ_m work function of the metal, E_F representing the Fermi level, $E_{vac,m}$ indicating the vacuum energy level of the metal, $E_{vac,d}$ denoting the vacuum energy level of the coating layer, $E_{K,F}$ representing the maximum kinetic energy of photoelectron excitation from the metal, $E_{K,C}$ indicating the maximum kinetic energy of photoelectron excitation from the dielectric, and ϕ_d representing the work function of the dielectric.

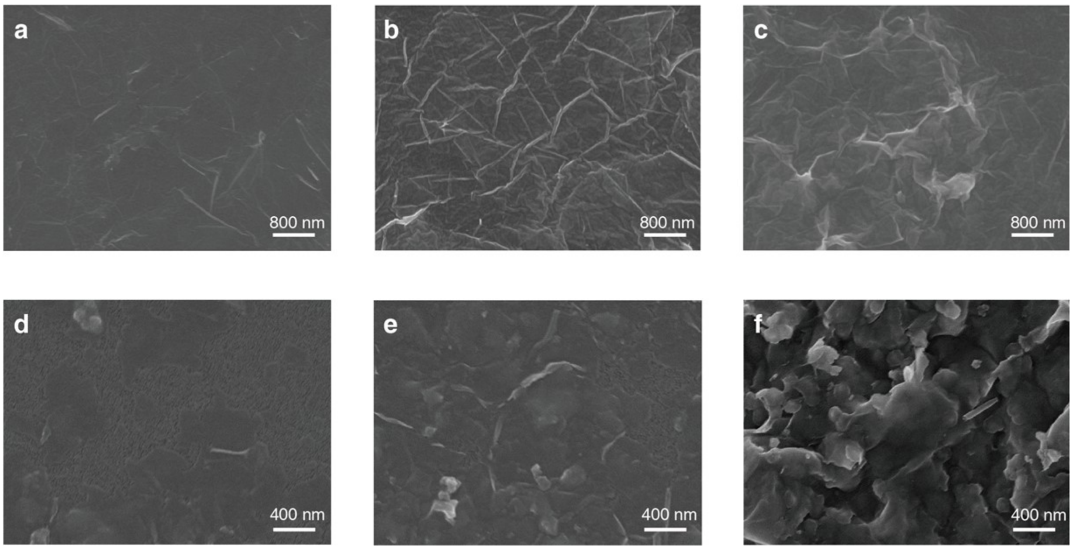

Figure S2. SEM images of PVDF films spray-coated with TiNS nanosheets at different concentrations: (a) 1 wt.%, (b) 5 wt.%, and (c) 10 wt.%. SEM images of PVDF films spray-coated with MMT nanosheets at different concentrations: (d) 5 wt.%, (e) 10 wt.%, and (f) 15 wt.%.

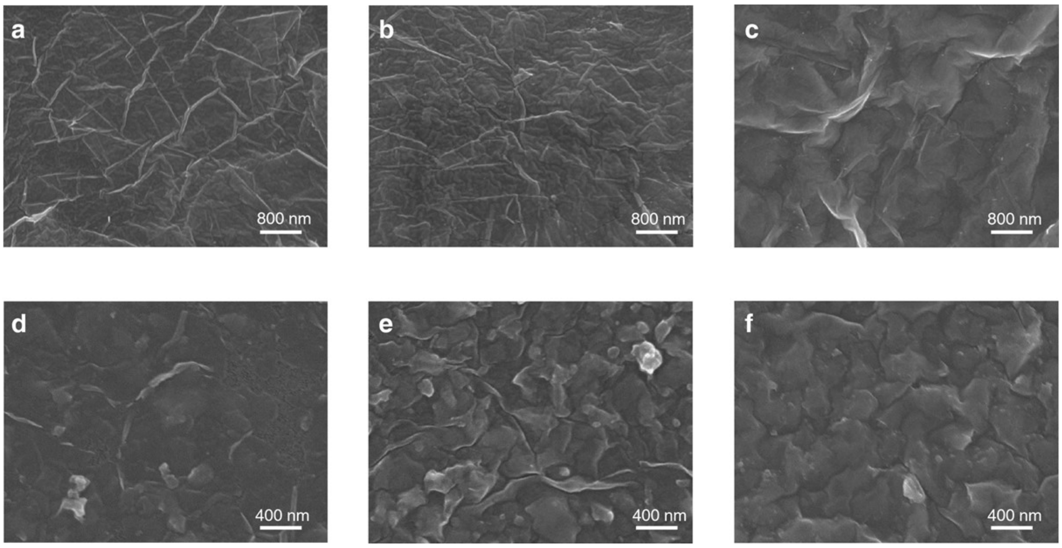

Figure S3. SEM images of (a) PVDF-TiNS1 (spray), (b) PVDF-TiNS2 (spray) and c) PVDF-TiNS3 (spray) films. SEM images of (d) PVDF-MMT1 (spray), (e) PVDF-MMT2 (spray) and (f) PVDF-MMT3 (spray) films.

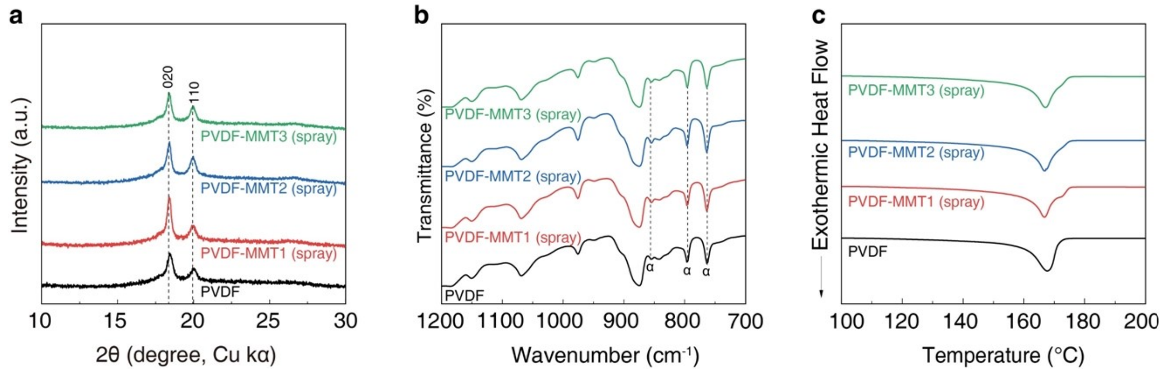

Figure S4. (a) XRD patterns, (b) FTIR spectra, and (c) DSC curves of pristine PVDF and PVDF-MMT (spray) films.

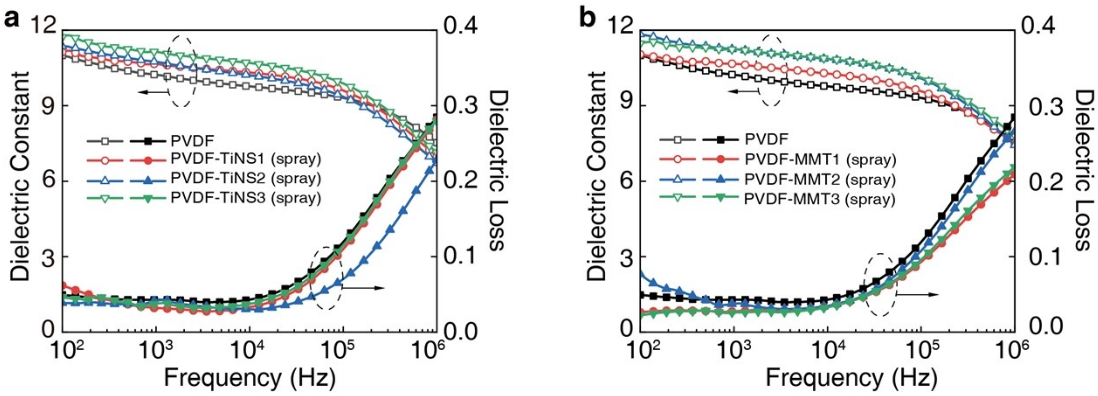

Figure S5. Frequency dependence of dielectric constant and dielectric loss of (a) PVDF-TiNS (spray) films and (b) PVDF-MMT (spray) films.

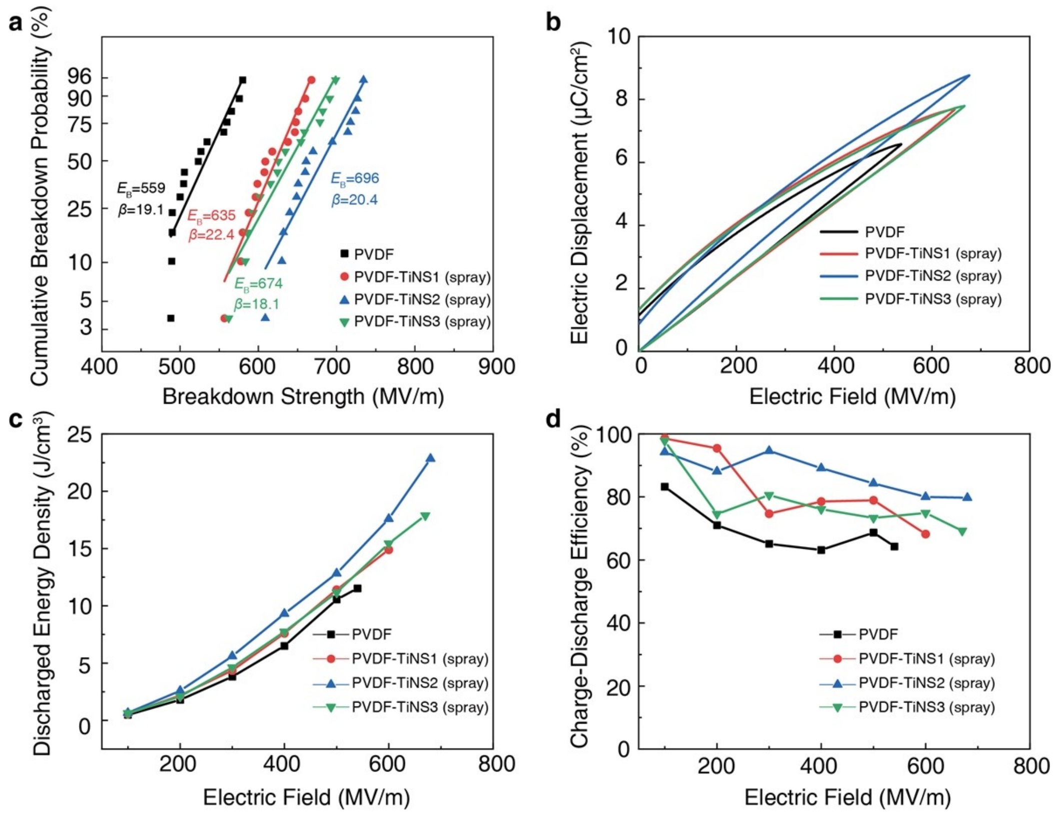

Figure S6. (a) Weibull breakdown strength of the PVDF-TiNS (spray) films. (b) Electric displacement-electric field loops obtained at 10 Hz. (c) Discharged energy density and (d) charge-discharge efficiency plotted as a function of electric field.

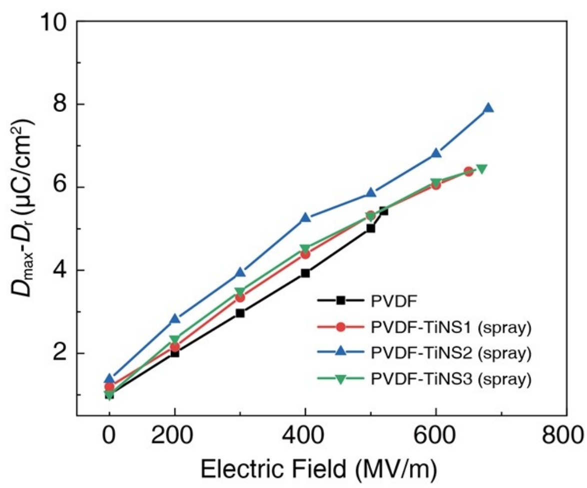

Figure S7. Variation of the D_{max} - D_r with the electric field for PVDF-TiNS (spray) films.

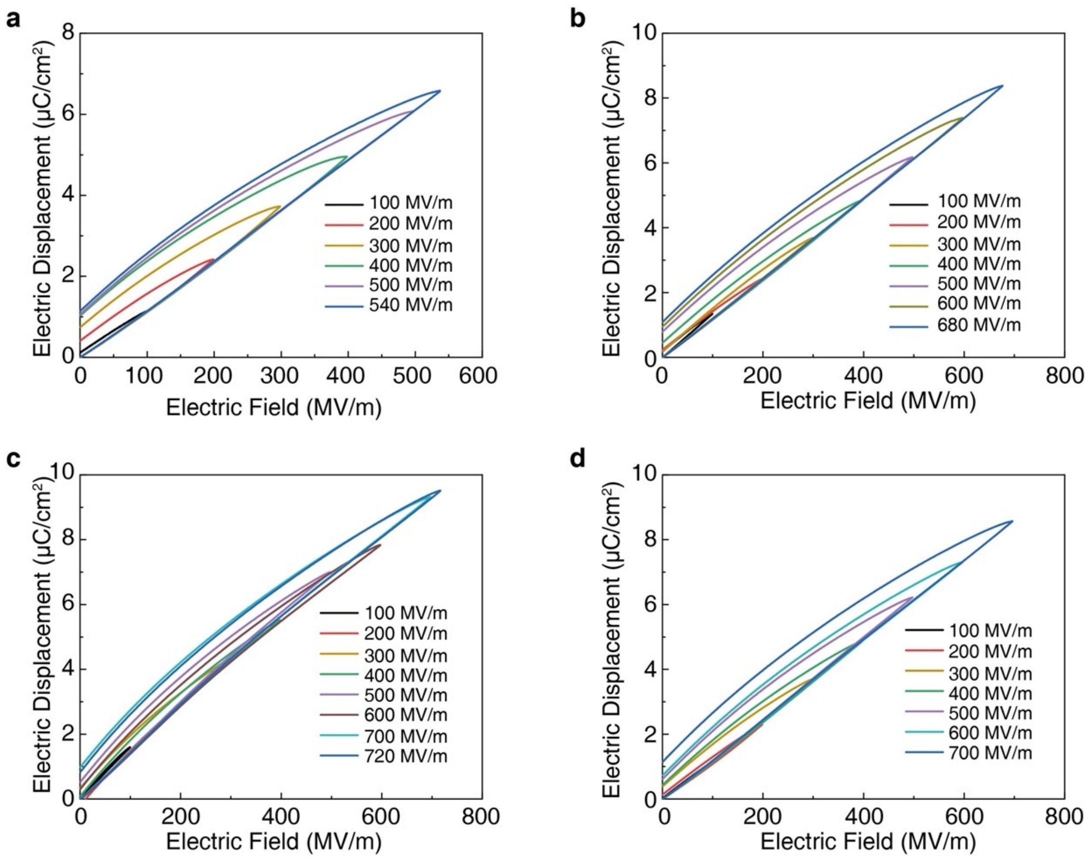

Figure S8. Electric displacement-electric field loops were collected at 10 Hz for (a) pristine PVDF, (b) PVDF-MMT1 (spray), (c) PVDF-MMT2 (spray), and (d) PVDF-MMT3 (spray) films.

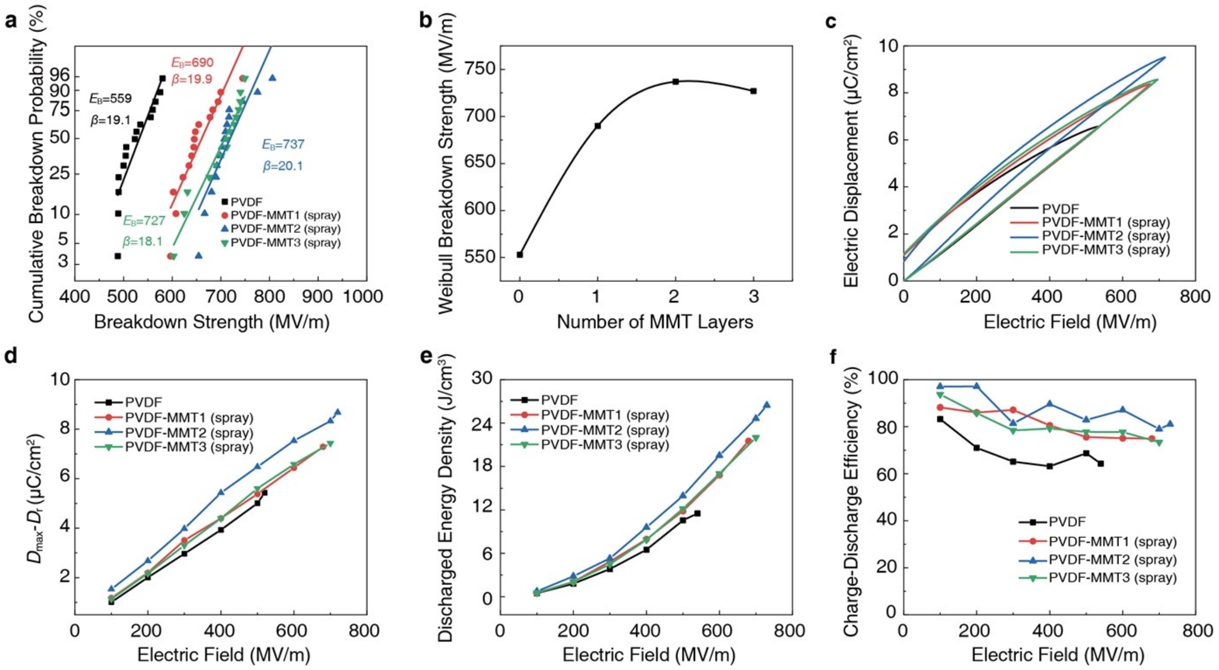

Figure S9. (a) Weibull statistic of breakdown strength of PVDF and PVDF-MMT series films. (b) Variation in Weibull breakdown strength as a function of the number of MMT layers. (c) Unipolar *D*-*E* loops collected at 10 Hz. (d) Variation of the D_{max} - D_r with the electric field for PVDF-MMT series films. (e) Discharged energy density and (f) charge-discharge efficiency as functions of electric field.

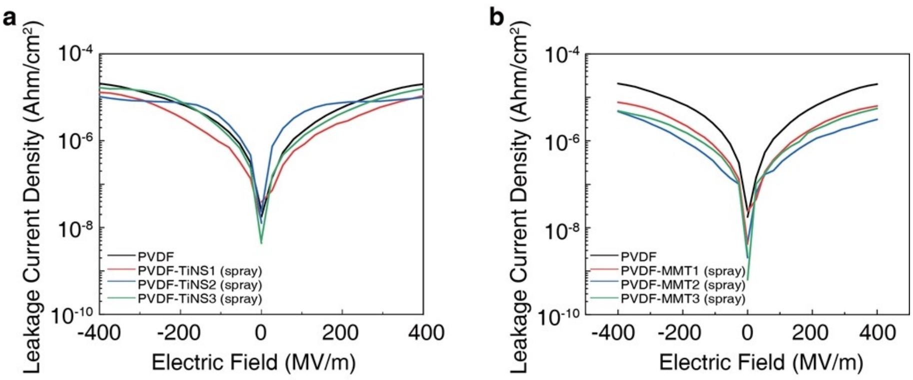

Figure S10. Leakage current density of PVDF-TiNS (spray) films and PVDF-MMT (spray) films.

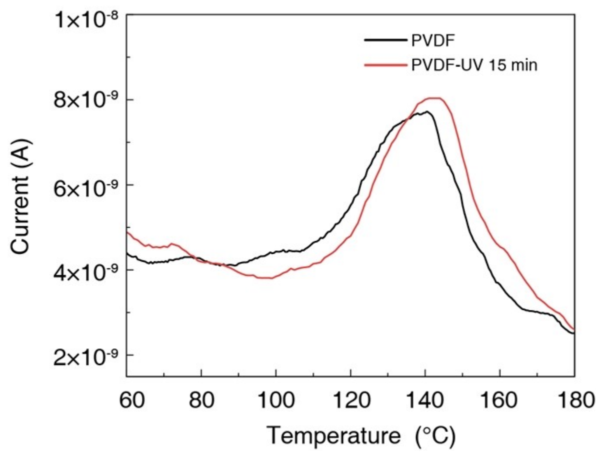

Figure S11. TSDC of PVDF and PVDF-UV 15 min films.

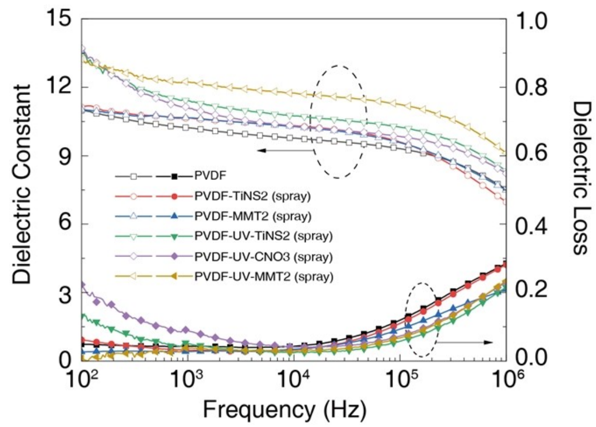

Figure S12. Frequency dependence of dielectric constant and dielectric loss of various polymer nanocomposite films.

Table S1. Comparison of energy storage properties in our work with other reported 2D nanofiller based single-layer nanocomposites.

Polymer	Filler	Content (%)	E_b (MV/m)	U_d (J/cm^3)	η (%)	Ref.
PVDF	$Ca_2Nb_3O_{10}$	0.9	792	36.2	61.2	[1]
PVDF	MMT	0.3	713	32.5	64	[2]
PVDF	BNNS	3.6	687	16.7	71	[3]
PVDF	BNNS	0.16	612	14.3	73	[4]
P(VDF-TrFE-CFE)	BNNS $Ti_{0.87}O_2$	1 3	660	20.8	73	[5]
PVDF	$BaTiO_3$ BNNS	/ 3	503	16.1	57	[6]
P(VDF-TrFE-CFE)	BNNS	18	742	32.5	62.4	[7]
PVDF	$Ti_{0.87}O_2$	1	650	21.2	67.9	[8]
PVDF	/	/	880	35	74	[9]
PVDF	/	/	880	39.8	72.8	[10]
PVDF	$Ti_{0.87}O_{2(spray)}$	/	680	22.8	79	This work
PVDF	$Ca_2Nb_3O_{10(spray)}$	/	720	26.4	80.4	This work
PVDF	$MMT_{(spray)}$	/	720	26.8	83	This work

Table S2. Comparison of energy storage properties in our work with other reported 2D nanofiller based multilayer-structured nanocomposites.

Polymer	Filler	Content (%)	E_b (MV/m)	U_d (J/cm^3)	η (%)	Ref.
PVDF	BNNS $Sr_2Nb_3O_{10}$	3 7	655	31.4	71	[11]
PVDF	BNNS SNO@BTO	12 9	651	32.5	64	[12]
P(VDF-HFP)	BNNS MoS_2	5 0.05	650	25	77	[13]
PVDF	SNO@Ag	5 7 9	585	31	66	[14]
PVDF	BNNS $Ba(Zr_{0.21}Ti_{0.79})O_3$	10 5	678	23.4	83	[15]
PVDF	$KNbO_3$ TiO_2	3 3	548	21.6	60	[16]
PVDF	BNNS $BaTiO_3$	10 8	588	20	60	[17]
PVDF	BNNS BTO@SiO_2	0.5 8	507	20.1	76	[18]
PVDF-UV	$Ti_{0.87}O_{2(spray)}$	/	700	25	75.8	This work
PVDF-UV	$Ca_2Nb_3O_{10(spray)}$	/	745	28.4	74	This work
PVDF-UV	$MMT_{(spray)}$	/	750	29.1	78.3	This work

References

[1] Z. W. Bao, C. M. Hou, Z. H. Shen, H. Y. Sun, G. Q. Zhang, Z. Luo, Z. Z. Dai, C. M. Wang, X. W. Chen, L. B. Li, Y. W. Yin, Y. Shen, X. G. Li, *Adv. Mater.*, 2020, **32**, 1907227.

[2] T. G. Zhu, H. Zhao, N. Zhang, C. Y. Zhang, L. Yin, Z. M. Dang, J. B. Bai, *Adv. Energy Mater.,* 2023, **13**, 2203587.

[3] J. S. Zhang, D. J. Hou, J. Wang, H. X. Liu, C. Huang, S. Cheng, L. Zhou, Z. H. Shen, B. W. Li, J. Zhou, P. C. Zhang, W. Chen, *ACS Appl. Mater. Interfaces,* 2024, **16**, 14162-14170.

[4] Y. K. Zhu, Y. J. Zhu, X. Y. Huang, J. Chen, Q. Li, J. L. He, P. K. Jiang, *Adv. Energy Mater.,* 2019, **9**,1901826.

[5] Y. N. Shang, Y. Feng, C. H. Zhang, T. D. Zhang, Q. G. Chi, *Compos. Part A-Appl. S.,* 2023, **167**, 107429.

[6] R. Guo, H. Luo, D. Zhai, Z. D. Xiao, H. R. Xie, Y. Liu, X. F. Zhou, D. Zhang, *Chem. Eng. J.,* 2022, **437**, 135497.

[7] J. Chen, Z. H. Shen, Q. Kang, X. S. Qian, S. T. Li, P. K. Jiang, X. Y. Huang, *Sci. Bull.,* 2022, **67**, 609-618.

[8] R. M. Wen, J. M. Guo, C. L. Zhao, Y. Q. Liu, *Adv. Mater. Interfaces,* 2018, **5**, 1701088.

[9] N. Meng, X. T. Ren, G. Santagiuliana, L. Ventura, H. Zhang, J. Y. Wu, H. X. Yan, M. J. Reece, E. Bilotti, *Nat. Commun.,* 2019*,* **10**, 4535.

[10] X. T. Ren, N. Meng, H. Zhang, J. Y. Wu, I. Abrahams, H. X. Yan, E. Bilotti, M. J. Reece, Nano Energy, 2020, **72,** 104662.

[11] H. R. Bai, K. Zhu, Z. Wang, B. Shen, J. W. Zhai, *Adv. Funct. Mater.*, 2021, **31**, 2102646.

[12] H. R. Bai, G. L. Ge, F. Yan, K. Zhu, J. F. Lin, C. Shi, J. Qian, Z. Wang, B. Shen, J. W. Zhai, *Energy Storage Mater.* 2022, **46**, 503-511.

[13] Y. Cheng, Z. B. Pan, H. R. Bai, H. X. Chen, L. M. Yao, X. P. Ding, S. H. Shi, J. J. Liu, Z. Y. Xie, J. K. Xu, J. W. Zhai, *ACS Appl. Mater. Interfaces,* 2022, **14**, 8448-8457.

[14] H. R. Bai, G. L. Ge, F. Yan, K. Zhu, J. Qian, C. Shi, Y. X. Li, H. J. Xie, B. Shen, J. W. Zhai, *Chem. Eng. J.*, 2023, **463**, 142428.

[15] J. Y. Jiang, Z. H. Shen, X. K. Cai, J. F. Qian, Z. K. Dan, Y. H. Lin, B. L. Liu, C.-W. Nan, L. Q. Chen, Y. Shen, *Adv. Energy Mater.*, 2019, **9**, 1803411.

[16] Y. Wang, L. L. Zhao, R. C. Chen, W. H. Zhao, D. W. Hu, H. R. Wang, B. Cui, *Nano Res.,* 2024, **17**, 4079-4088.

[17] F. H. Liu, Q. Li, J. Cui, Z. Y. Li, G. Yang, Y. Liu, L. J. Dong, C. X. Xiong, H. Wang, Q. Wang, *Adv. Funct. Mater.*, 2017, **27**, 1606292.

Q. Z. Sun, J. P. Wang, H. N. Sun, L. Q. He, L. X. Zhang, P. Mao, X. X. Zhang, F. Kang, Z. P. Wang, R. R. Kang, L. Zhang, *Compos. Part A-Appl. S.,* 2021, **149**, 106546.